Mapping of Micro Topography on Hill Slopes Using Airborne Laser Scanning

Tatsuo SEKIGUCHI,[1] Hiroshi P. SATO,[2] Seiji ICHIKAWA,[1] Ryoichi KOJIROI[2]

Abstract

Rain-induced landslides may result in disaster by destroying homes and buildings. Fluid landslides are characterized by rapid movement and long run-out distance. Aerial photos have been used to observe and measure the slopes. In addition, a new technology called airborne laser scanning, is a promising tool for observing and measuring slopes. In this study, hilly terrain where landslides have occurred was measured by airborne laser scanning. Furthermore micro landslide characteristics such as scars were identified in detail, by combining contour maps based on airborne laser scanning data and remote sensing such as aerial photos interpretation.

1. Introduction

Japan has many hills and mountains, and it is located in humid climate influenced by the wet monsoon. Rain-induced landslides may cause disasters by destroying homes and buildings in urban and urbanizing areas. Fluid landslides, which are most dangerous and damaging, are characterized by rapid movement and long run-out distance (Wang and Sassa, 2002). To elucidate the mechanism of this phenomenon, it is important to measure slopes which have already caused landslides in detail. Photogrammetry has been frequently used for the measurement. In addition, it has become possible to use a new technology called, airborne laser scanning for three-dimensional measurement in detail.

Airborne laser scanning has begun to be used to identify landslide characteristics (Hasegawa and Okamatsu, 2001; Sato et al, 2002). It is expected that airborne laser scanning will accelerate not only high-precision mapping but also landform analysis in detail. In other words, high-precision topographic maps, elevation tint maps, slope tint maps and shading maps will be produced more efficiently. Furthermore, micro topography mapping, calculation for landslide simulation and unstable slopes identification will be actively performed. The purpose of this study is to show the example of the mapping hilly terrain and micro topography by airborne

[1] Disaster Prevention Geography Division, Geographic Department
[2] Geographic Information Analysis Research Division, Geography and Crustal Dynamics Research Center

laser scanning data measured in Tama Hills near Tokyo.

2. Study area

The Tama Hills are located near the boundary between the western Kanto Mountains and the Kanto Plain (Fig. 1). The Tama Hills lie on the southwest side of the Tama River, and elevation gradually increases from the southeast to northwest. Namely, the elevation increases from 80 m in the eastern part of Kawasaki and Yokohama to 200 m at Hachioji City.

Though many rivers dissect the hills, the profile is generally gentle (Fig. 2). The northeastern part of the Tama Hills, which is closest to Tokyo, has rapidly urbanized and it is difficult to find the original scenery there.

3. Data preparation

3.1 Airborne laser scanning

An airborne laser scanning is an active sensor that measures the distance from the sensor to the ground on which the laser beam is reflected (Fig. 3). However, the distance data alone cannot give the ground position. With high accuracy aircraft position is calculated using a combination of Global Positioning System (GPS) data both on the aircraft and on the ground, and aircraft acceleration and three-axial attitude (ω, ϕ, κ) data measured by Inertial Measurement Unit (IMU). Furthermore, direction data of laser beam are measured in the sensor onboard. These data are combined to calculate the three-dimensional position (X, Y, Z) on the ground is calculated. For more information about airborne laser scanning, refer to Ackermann (1999)
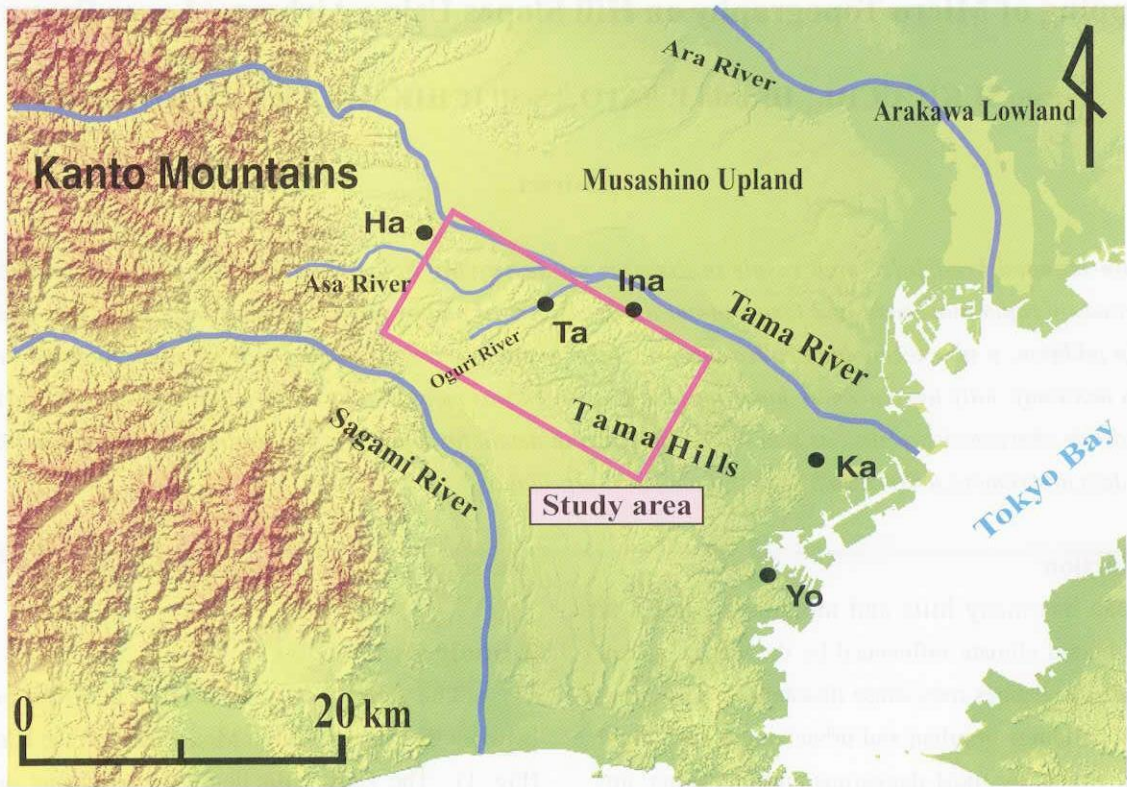
Fig. 1 Study area (Geographical Survey Institute (GSI)'s 50 m grid DEM was used.)
Note: Ha: Hachioji City; Ta: Tama City; Ina: Inagi City; Ka: Kawasaki City;
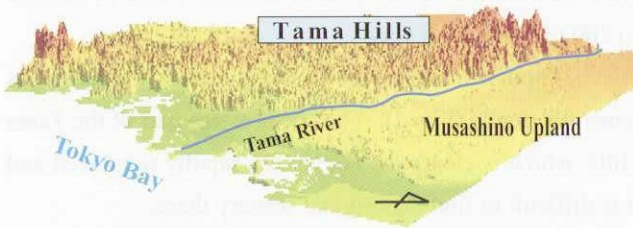Yo: Yokohama City.

Fig. 2 Profile the Tama Hills, made by GSI's 50 m grid DEM.

and other articles in the same issue of the ISPRS Journal of Photogrammety and Remote Sensing.

In the study area, high-density and high-precision laser data were obtained for the Kawasaki, Inagi and Hachioji sub-areas in December 2001. Measurement areas were 6 km² in total. In this study, the measurement specifications were as follows; laser instrument, EnerQuest RAMS system; laser wavelength 1064 nm; pulse rate 24000 Hz; scanning frequency 24 Hz; flying altitude, nominally 2600 m above the ground; flight speed 203.7 km/h; swath width 881 m. The interval of the measurement points was 2.5 m in the track direction and 2.0 m in the cross direction. In each sub-area six flight courses were in the east-west direction and four flight courses were in the
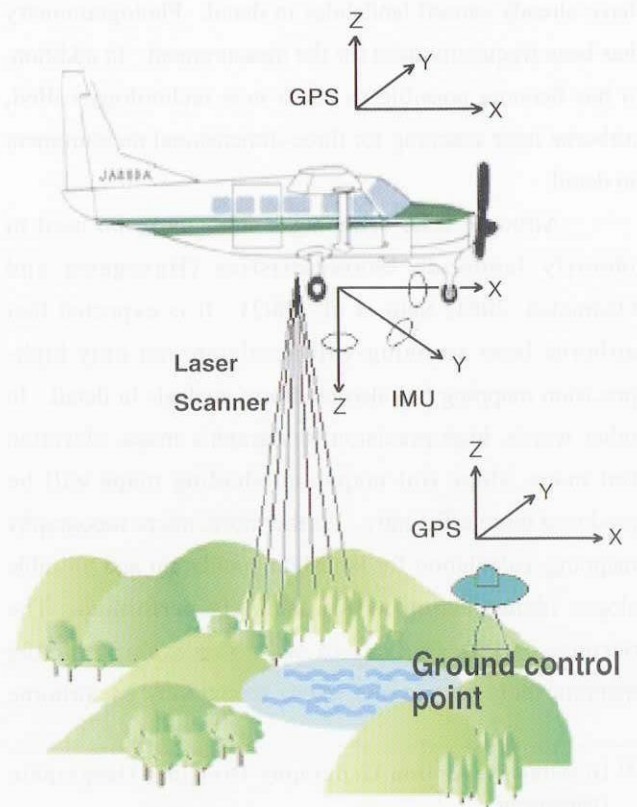

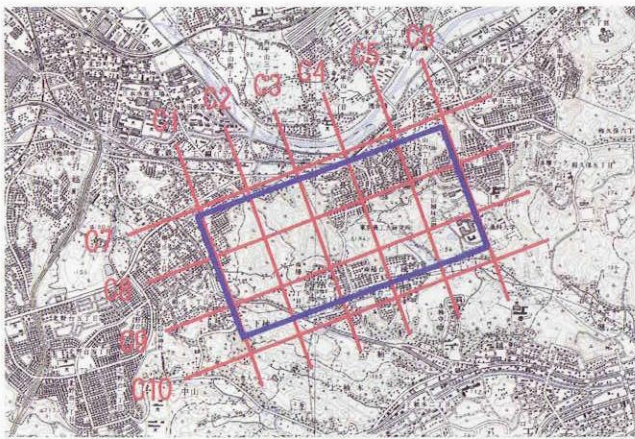**Fig. 3** Measuring principle of airborne laser scanning.

Fig. 4 Flight course in the study area.
Note: Red line: Flight course; A area delineated by
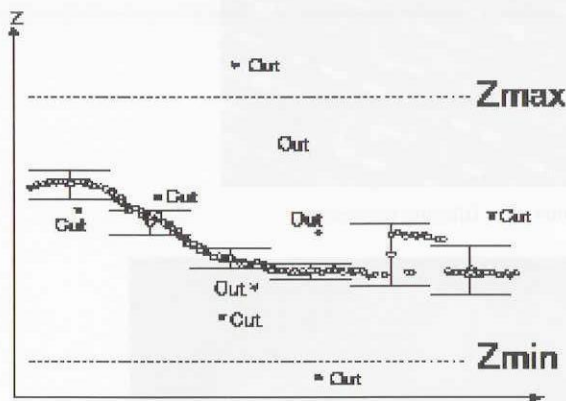Blue line: Hachioji sub-area.

Fig. 6 DSM and DTM (Masaharu et al., 2000).

Fig. 5 Noise data deletion.
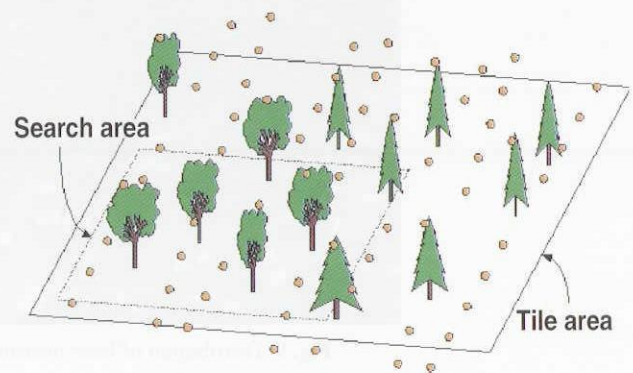
Fig. 7 Filtering processing (1).

Fig. 8 Filtering processing (2).

north-south direction (Fig. 4). As a result, each sub-area had 10 flight courses. The aircraft flew each course only once. The course interval was 400 m and the course overlap was 54.6 %.

A 1 m by 1 m grid was laid on each sub-area and the number of grids that contained at least one laser measurement point was counted. The ratios of the number of those grids to the total number of grids were 87 %, 92 % and 91 % in Kawasaki, Inagi and Hachioji sub-area, respectively.

3.2 Noise processing

Laser measurement points which indicate extremely high or low elevation were removed by comparing elevations on laser measurement points with existing contour maps (Fig. 5). Next, the average value and standard deviation σ of elevation on laser measurement points in 25 m by 25 m areas were calculated, and laser measurement points whose absolute value of deviation in
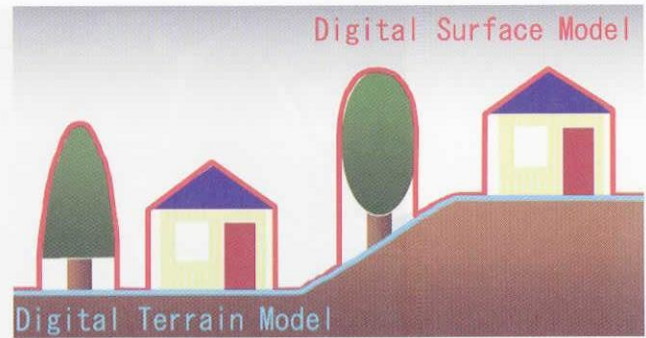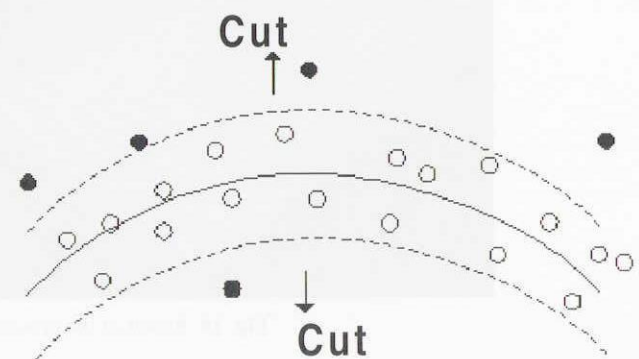
elevation were over σ were removed.

As a result, a Digital Surface Model (DSM) was obtained. DSM consists of both the surface of the ground and ground features such as buildings and trees, but in this step the DSM consisted of randomly scattered laser measurement points.

3.3 Filtering

To show only the surface of the ground, namely, Digital Terrain Model (DTM), it is necessary to remove the surface of ground features from the DSM (Fig. 6) by filtering (Figs. 7 and 8).
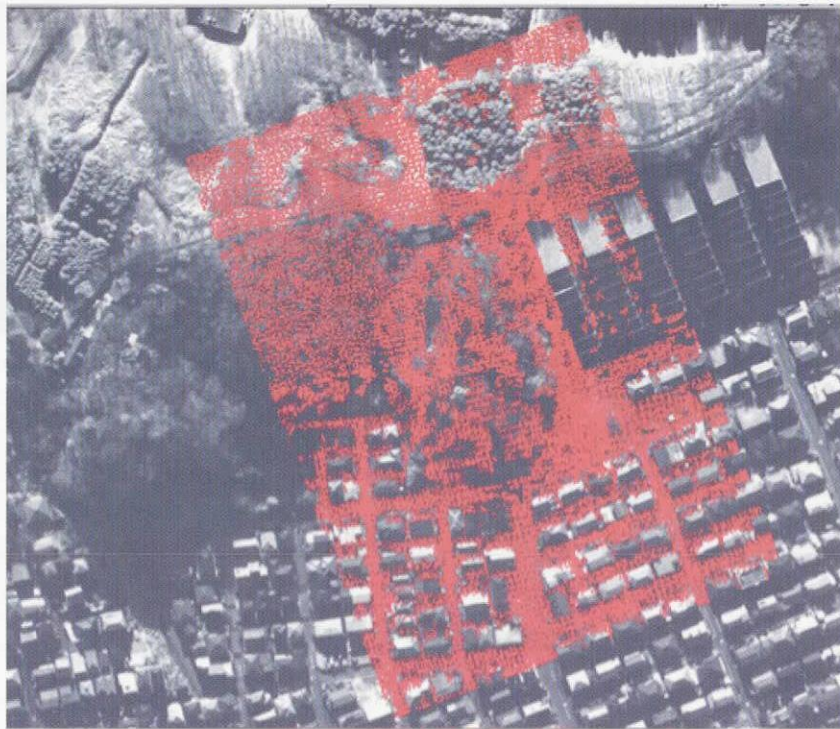
Fig. 9 Distribution of laser measurement points after filtering processing.
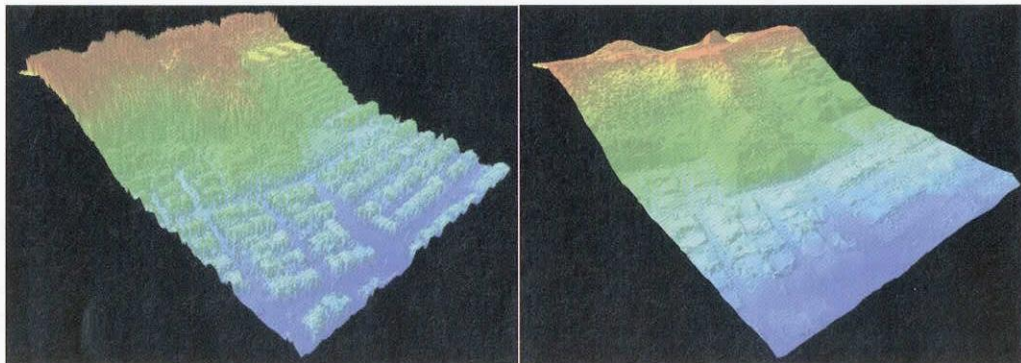

Fig. 10 Result of the processing (left : before ; right : after).

First, 1 km by 1 km tile area was fixed over the study area (Fig. 7). Next, in the tile area, search area at the size of from 18 m by 18 m to 50 m by 50 m was shifted at the overlap of 25 % in area (Fig. 7). Laser measurement points in each search area were approximated by polynomials of degree two (Fig. 8), which gave a threshold value from 2 m to 9 m. Finally, laser measurement points over the threshold value were eliminated from the search area. After this processing, the 1 km by 1 km tile area was shifted at the overlap of 25 % in area, search area at the size of from 18 m by 18 m to 50 m by 50 m was shifted in the tile area, and the same processing was performed to obtain smooth DTM. The above process was automatically performed three times.

Furthermore, manual processing was performed to obtain smoother DTM. In this step, the DTM consists of randomly scattered laser measurement points. In advance, a contour map was drawn on a Triangulated Irregular Network (TIN) calculated by the DTM, and the contour map was superimposed on an orthogonal color aerial photo. When the contour lines were dense on buildings or trees on the superimposed image, laser measurement points where the contour lines were dense were removed from the DTM. The manual processing was repeated three times to produce a more realistic DTM on the superimposed image.

In this step, the DTM consists of randomly scattered laser measurement points. As an example, distribution of the points is shown in Fig. 9. The results of

the filtering processing are shown in Fig. 10.

3.4 Validation of DTM elevation measurement accuracy

To validate DTM elevation measurement accuracy, DTM was compared with existing 1 : 500 scale photogrammetric contour maps at the contour interval of 1 m (Unozawa and Oka, 1972). Here, elevation measurement accuracy in Kawasaki sub-area is discussed.

First, two validation lines were selected on ridges and valleys on the photogrammetric contour map. Next, in each line two types of cross sections were prepared (Fig. 11): one was plotted based on the photogrammetric contour map and the other was calculated based on the laser DTM obtained in the preceding section.

In the former plotting, plane position (x, y) and elevation h were measured at the cross between the validation line and the photogrammetric contour line. In the latter calculation, the plane position (x, y) was interpolated to the DTM to obtain elevation H. Two interpolation methods were tried: elevation H_1 was obtained on TIN and elevation H_2 was obtained by the Inverse Distance Weighted (IDW) method. Finally, h was compared with H_1 and H_2 in the plane position (x, y) to validate DTM elevation measurement accuracy. As a result, in the validation lines, standard deviation of $(H_1–h)$ was 0.6 m or 1.6 m on the ridge and 0.8 m or 1.2 m on the valley, respectively. And standard deviation of $(H_2–h)$ was 0.5 m or 1.6 m on the ridge and 0.9 m or 1.2 m on the valley, respectively.

A assuming that h is the "real" elevation on the ground, DTM elevation measurement accuracy was
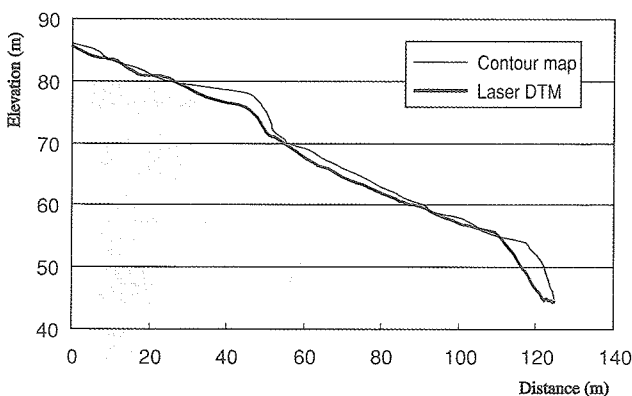
validated between 0.5 m and 1.6 m in standard deviation. There seemed to be little difference between the two interpolation methods. Furthermore, it was found that h was lower than H_1 and H_2 on the ridge and higher than H_1 and H_2 in the valley.

3.5 Contour map

A contour map of the study area was drawn on DTM. First, TIN was calculated by DTM. In this step, the DTM consisted of randomly scattered laser measurement points. Next, 1 m, 2 m and 5 m grid DTMs were obtained from the TINs. In this step, the DTMs consisted of regularly arranged points, namely, grid data. Then contour maps of 1 m, 2 m and 5 m contour intervals were drawn on the respective grid DTM. Finally, nine kinds of contour maps (three kinds of grid intervals by three kinds of contour intervals) were produced. In terms of smooth contour lines, micro topography expression and ease of landform interpretation, it was found that the 2 m interval contour map made from 2 m grid DTM was the best contour map of the study area.

This contour map of the Hachioji sub-area called a laser contour map in this study is shown in Fig. 12. Fig. 13 is a photo-grammetric contour map. These two maps show the same place at the same scale. The laser contour map shows contour lines very clearly, and describes ridges and valleys more realistically than the photogrammetric contour map.

3.6 Various mapping expression methods using airborne laser scanning data

In the study area, it is possible to interpret landform characteristics on laser contour maps. In addition to contour maps, there are many methods for expressing landforms, such as slope tint maps, elevation tint maps and shading maps. Shading maps give us stereoscopic vision. Image of elevation tint map superimposed on shading map (Fig. 14) was found to be helpful to know landform approximately, because relief is visually comprehensible. In Fig. 14, the lower the elevation is, the bluer the color is, and the higher the elevation is, the redder the color is. And in the figure, the light is given from the fixed height and direction and shade is cast on the ground.
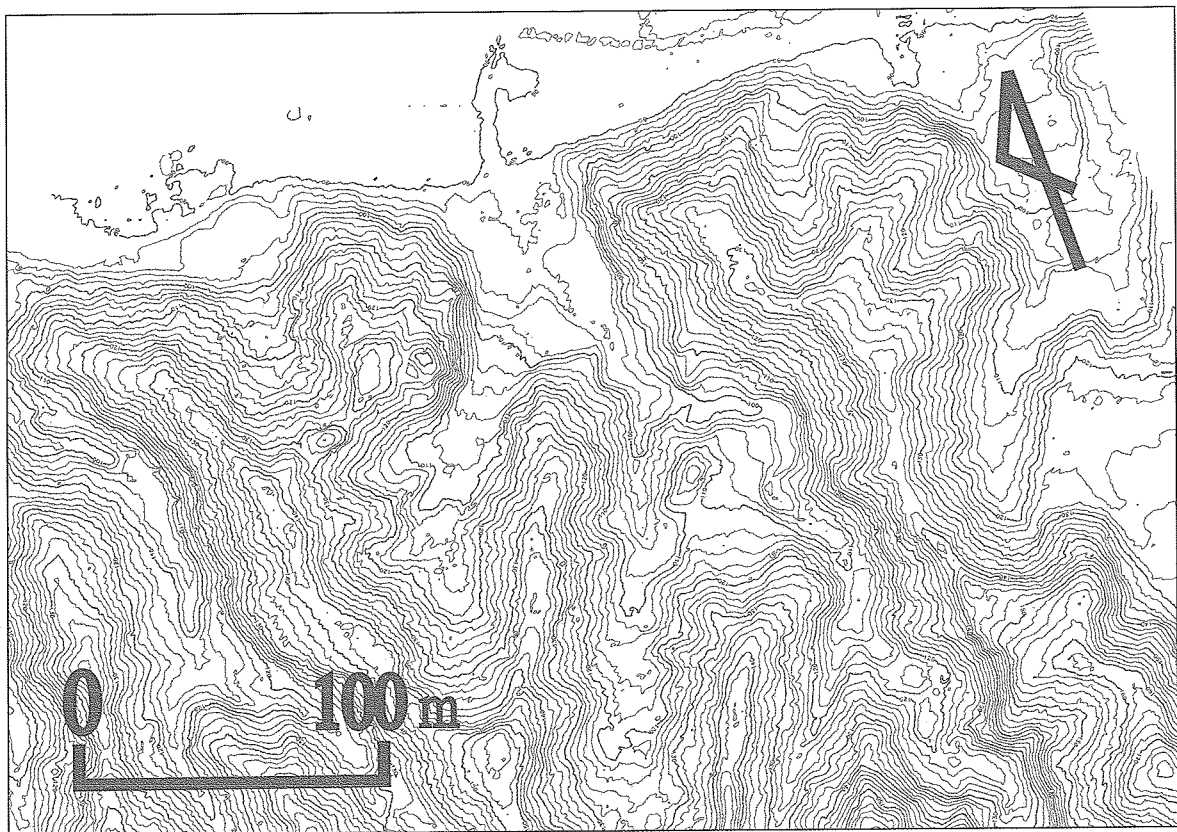

Fig. 11 Overlap of cross sections based on a photogrammetric contour map and laser DTM (Kawasaki sub-area).

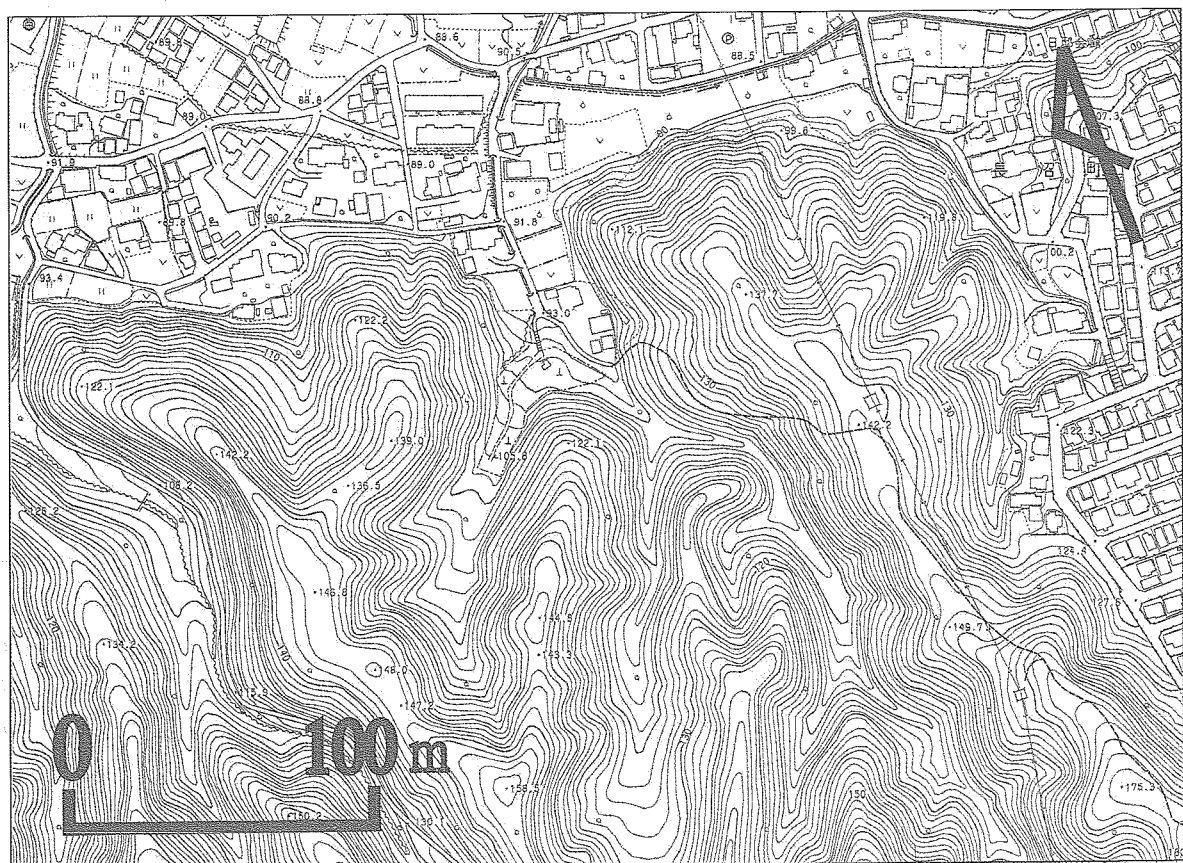**Fig. 12** 2 m interval contour map based on a 2 m grid DTM (Hachioji sub-area).

Fig. 13 1: 2,500 photogrammetric contour map (Tokyo city planning map, 1999).
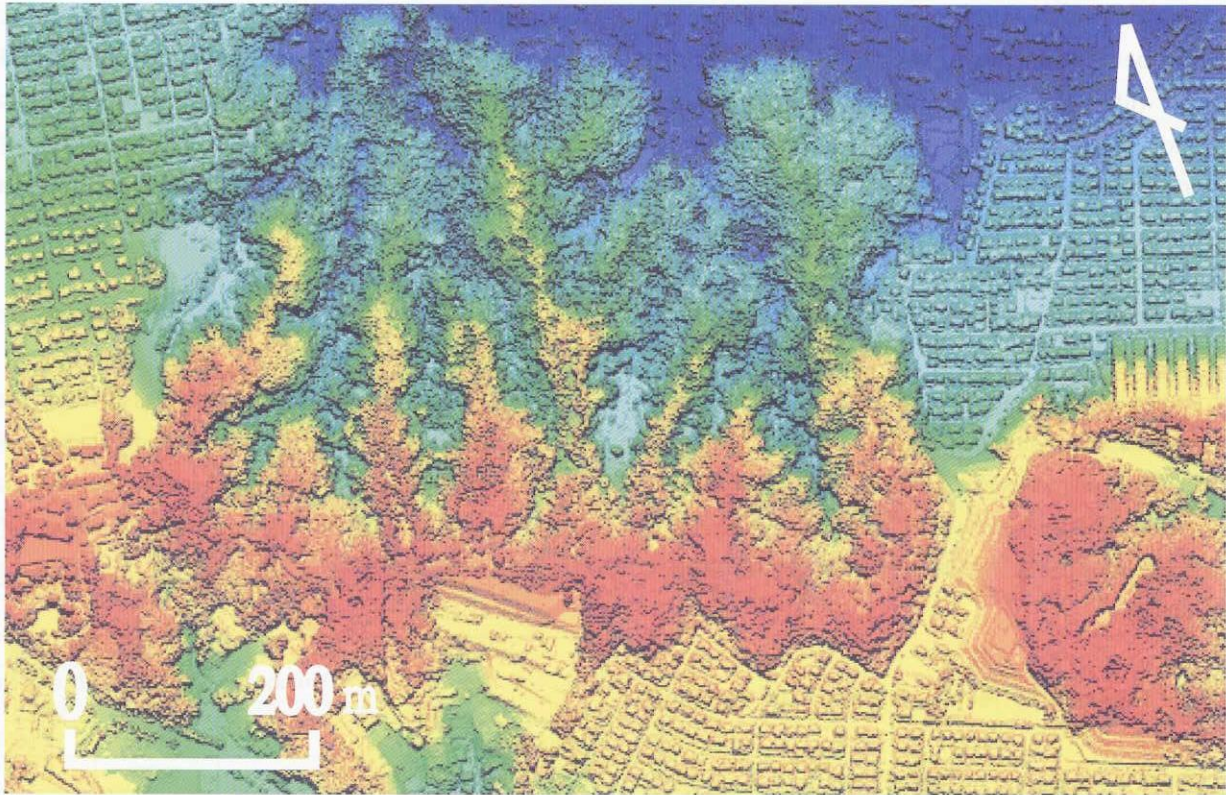
Fig. 14 Image of elevation tint map superimposed on shading map based on DSM (Hachioji sub-area).

Image processing software ERDAS IMAGINE was used to produce Fig. 14.

4. Micro topography extraction by airborne laser scanning data

4.1 Landform and geology of the Tama Hills

In Fig. 15, the Tama Hills extend from near Tokyo Bay to the Kanto Mountains. Though there are few flat surfaces on the northwestern part of the hills, many ridges and valleys exit. In the central and the southern parts of the hills, elevation decreases and flat surfaces are wide in area.

The Tama Hills have been classified as Tama I and Tama II surfaces according to the kind of Kanto loam that underlies them (Hatori and Juen, 1958; Unozawa and Oka, 1972; Oka, 1991; Kaizuka et al., 2000). Tama II surface is located on the south side of Tama I surface. Generally, the Tama I ridge extends from east-northeast to west-southwest, and the closer the ridge is to the Tama River, the lower is its elevation. The Tama II ridge runs from east to west, and the closer the ridge is to Tokyo Bay the lower is its elevation, generally.
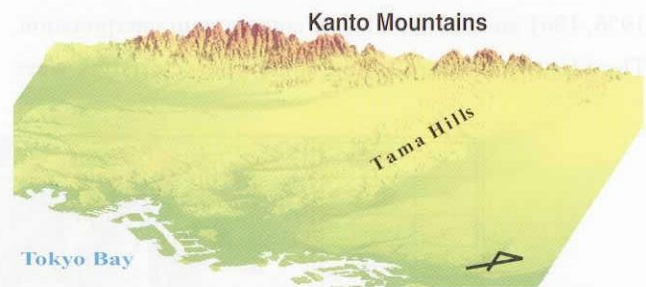

Fig. 15 An air view on the Tama Hills, made by GSI's 50 m grid DEM.

The Tama Hills bedrock consists of Early Pleistocene series of sand and mud alternation strata. The series underlies Gravel layer (Hatori and Juen, 1958). The gravel layer was deposited in the alluvial fan formed by the old Sagami River in the Middle Pleistocene age (Kaizuka et al., 2000). Next, Tama loam layer, which is a Kanto loam layer, overlies the gravel layer (Hatori and Juen, 1958; Unozawa and Oka, 1972; Oka, 1991; Kaizuka et al., 2000).

In the Hachioji sub-area, the Oguri River flows east-southeast, through the south side of the sub-area. The Asa River flows east through the north side of the sub-area. The relief between the Tama I ridge and the Oguri River

bed is less than the relief between the Tama I ridge and the Asa River bed. Branches of the Oguri River, whose valleys are wide and shallow, incise the southern slopes in the Hachioji sub-area. Branches of the Asa River, whose valleys are narrow and deep, incise the northern slopes in the sub-area. The south part of Tama I surface has been remarkably eroded.

In the Hachioji sub-area, the southern has been heavily urbanized. The northern part, where many natural slopes remain, consists of steep valley walls with narrow valley bottoms and gentle slopes on the ridge. There are two knick lines: one is located near the ridge and the other is located on the slope bellow that. Here, "knick line" means a convex break of slope where gentle slopes become steep.

4.2 Micro topography identification in the Hachioji sub-area

Micro topographic characteristics in the northern slopes in the Hachioji sub-area were identified by a combination of multi-temporal aerial photos, taken in 1956, 1961 and 1974, and laser contour map interpretation. The identified micro topographic characteristics were overlapped on a laser contour map, to create the micro topography classification map shown in Fig. 16. Here, ridges and valleys extend from south-southwest to north-northeast. It was found that laser contour maps reflect landforms more realistically than photogrammetric contour maps.

4.3 Slope failure and landslide characteristics in the Hachioji sub-area

To make the micro topography classification map in Fig. 16, many slope failure and landslide characteristics were continuously confirmed by multi-temporal aerial photo interpretations. It was surmised that slope failures

Table 1 Results of the landslide scar extraction on laser contour map

Item	Number	Occurred Position	
		Knick Line (%)	Except Knick Line (%)
Slope Failure in 1956	3	1 (33)	2 (66)
Slope Failure in 1961	12	5 (42)	7 (58)
Slope Failure in 1974	14	5 (36)	9 (64)
Old Slope Failure	12	9 (75)	3 (25)
Landslide	12	12 (100)	–
Total Counts (%)	53	32 (60)	21 (40)

Note: This table was produced by the combination of interpretations on laser contour map and multi-temporal aerial photos.
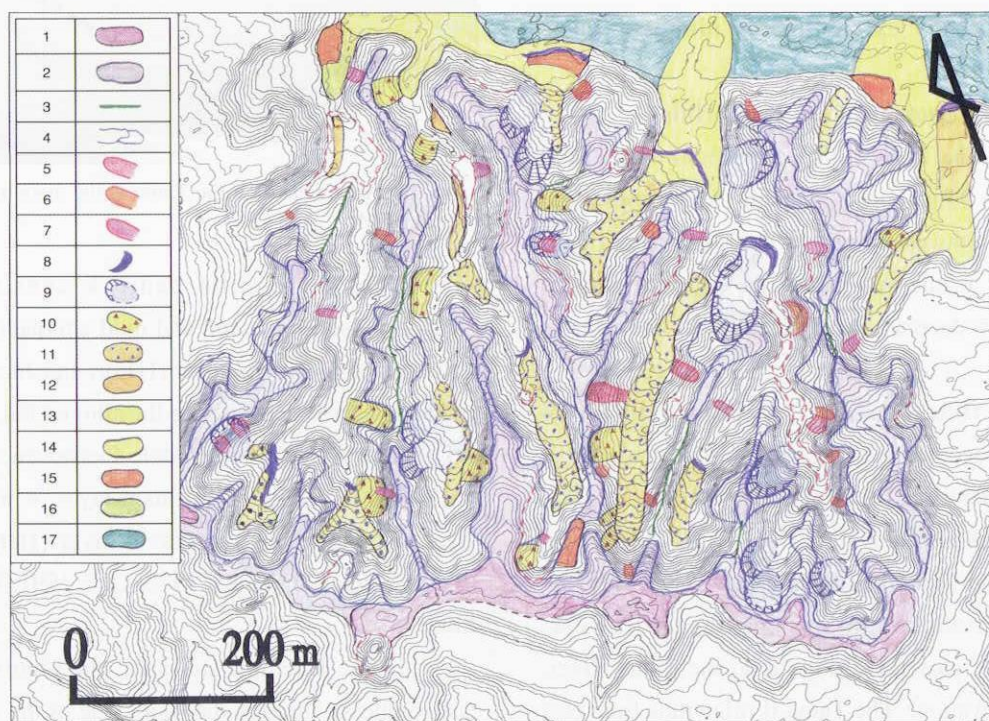

Fig. 16 Micro topography classification map overlapped on a laser contour map (Hachioji sub-area).
Note: The code for each item corresponds to the code in Table 2. Areas in broken lines show where the laser contour map does not indicate realistic landform.

may actively occur there.

As shown in Fig. 16, knick lines are formed along ridges and valleys. Slope failures extend cross wide to ridges and valleys. Slope failures were confirmed at 3, 12 and 14 places in 1956, 1961 and 1974, respectively (Table 1).

All landslides occurred at knick lines near the ridge. The geology near the knick lines is Tama loam underlain by Middle Pleistocene series such as gravel layers (Fig.
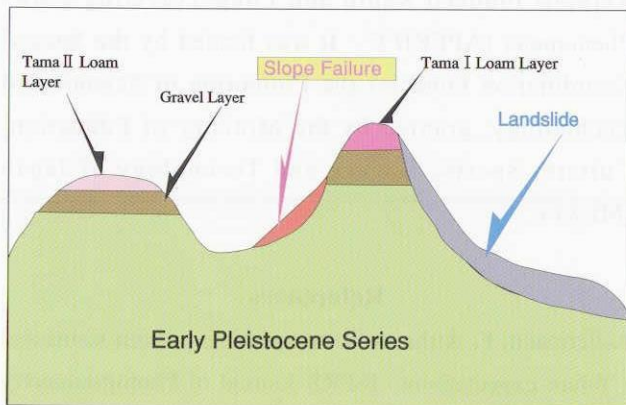

Fig. 17 Schematic cross section of slope failures (Hachioji sub-area).

17). Many slope failures have occurred at knick lines on the hill. The geology of the mid-slope is Middle Pleistocene series such as gravel layer underlain by Early Pleistocene series such as alternating sand and mud strata.

4.4 The effectiveness of airborne laser scanning data for landslide study

As shown in Figs.12 and 16, laser contour maps indicate micro topographic characteristics clearly and realistically. Laser contour maps are also useful than photogrammetric contour maps to place and delineate slope failures, landslide scars and other micro topographic characteristics interpreted on aerial photos. However, laser contour maps do not always indicate realistic landforms: a few errors were confirmed on valley bottoms or near ridges (refer to the footnote of Fig. 16 for details). According to detailed field survey and aerial photo interpretation, bamboo grasses grew thick in the valley bottom and needleleaf evergreen trees such as cedar covered the ground densely near the ridge (Fig. 18).

Table 2 Items on micro topography classification maps

Code	Micro Topography	Legend	Charaicteristics	Interpretation
1	Summit Flat Surface		Flat surface in the summit (Gravel Layer and Tama Loam Layer Surfaces)	△
2	Summit Gentle Slope		A little gentle slope comparing summit flat surface (Gravel Layer and Tama Loam Layer Surfaces)	○
3	Ridge		Ridge by erosion and slope failure insid slope (Early pleistocene series)	○
4	Knick Line		The line where gentle slope changes to steep slope	○
5	Slope Failure in 1956		Slope failure interpreted 1956 aerial photo	●
6	Slope Failure in 1961		Slope failure interpreted 1961 aerial photo	●
7	Slope Failure in 1974		Slope failure interpreted 1974 aerial photo	●
8	Cliff		River terrace cliff and cliff in the valley	△
9	Landslide		Landslide	△
10	Talus		Steep slope failure and steep inclination landslide	●
11	Debris Avalanche		Alluival deposit surface in the valley plain	△
12	Debris Avalanche Terrace		Terrace formed by debris avalanche valley	●
13	Alluvial Cone		Alluival fan formed steep and small size of alluvial fan	○
14	Alluvial Fan		Genttle slope and big size alluvial fan	○
15	River Terrace		Terrace and platform along to the river	○
16	Valley Plain		Flat plain of the valley in which the width is wider than debris avalanche	○
17	Flood Plain		Flat plain and lowland	○

Note: Clearness of interpretations using laser contour maps.
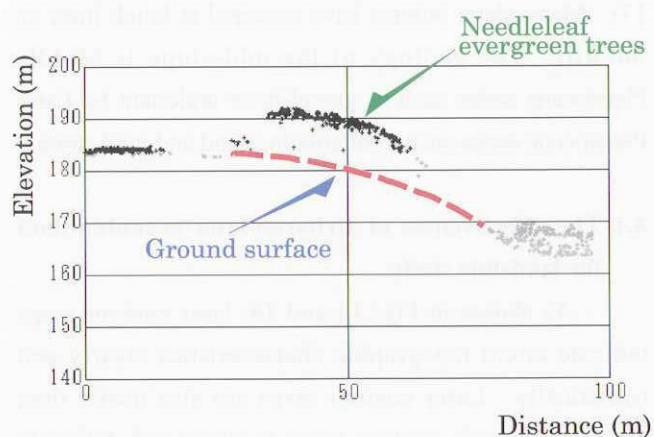○: Very clear; △: Clear; ●: Unclear.

Fig. 18 Cross section of elevation data measured by airborne laser scanning (Hachioji sub-area).

5. Conclusion

Airborne laser scanning was carried out on the Tama Hills to obtain laser data with which to produce contour maps. It was found that laser contour maps indicate landforms such as knick lines and landslide scar more realistically than photogrammetric contour maps.

It was also found that the laser contour map at the contour interval of 2 m, produced by 2 m grid DTM, was useful for interpreting micro topographic characteristics. With multi-temporal aerial photo interpretations, micro topographic characteristics including slope failures, and landslides were identified. The identified features were placed or delineated on a laser contour map to produce a micro topographic classification map. The classification map indicated that many slope failures have occurred at knick lines on the hills.

There are many methods for expressing landforms. Slope tint maps, elevation tint maps, shading maps and images of elevation tint map superimposed on shading map were also produced by the laser data. Shading maps give us stereoscopic vision, and landform relief is comprehensible by the images of elevation tint maps superimposed on shading map.

In the future, it will be necessary to study how to identify relatively high-risk places for slope failures using laser data, micro topographic classification maps and field survey data. It will also be necessary to examine the relation between ground cover ratios and the distribution of laser measurement points of DTM.

References

Ackermann, F, Airborne laser scanning–present status and future expectations. ISPRS Journal of Photogrammetry and Remote Sensing, 54, 64-67, 1999.

Hasegawa, H. and K. Okamatsu, Detailed landform feature and characteristics extraction with high dense DTM data. Proceedings of the autumn conference of the Japan Society of Photogrammetry and Remote Sensing, JSPRS, 189-192, 2001. (in Japanese)

Hatori, K. and S, Juen, The Quaternary history of the western margin of Kanto basin (I), (II). The Journal of the Geological Society of Japan, 64, 181-194, 232-349, 1958. (in Japanese with English abstract)

Kaizuka, S., K. Koike, K. Endo, H. Yamazaki and T. Suzuki, *Landforms, no.4, Kanto and Izu Ogasawara.* 349p, 2000. University of Tokyo press. (in Japanese)

Masaharu, H., H. Hasegawa and K., Ohtsubo, Extraction of buildings from laser scanner DSM by using normalized DSM. Proceedings of the 29th Conference of the Remote Sensing Society of Japan, 239-240, 2000. (in Japanese)

Oka, S., Geology of Middle-Upper Pleistocene series in southwestern Kanto district. Bulletin of Geological Survey of Japan, 42, 553-653, 1991. (in Japanese)

Sato, H. P., H. Hasegawa, K. Okamatsu and H. Masaharu, Landslide Topography Measurement by Airborne Laser Scanning. Proceedings of international symposium on Landslide Risk Mitigation and Protection of Cultural and Natural Heritage, 375-383, 2002. UNESCO and Kyoto

University.

Unozawa, A. and S. Oka (eds), 1:10,000 Geological map of Kwanto loam beds in north western part of Tama Hill. 1972. Geological Survey of Japan. (in Japanese)

Wang, G. and K. Sassa, Pore pressure generation and motion of rainfall-induced landslides in laboratory flume tests. Proceedings of international symposium on Landslide Risk Mitigation and Protection of Cultural and Natural Heritage, 45-60, 2002. UNESCO and Kyoto University.